Published in final edited form as:
Cancer Prev Res (Phila). 2011 June ; 4(6): 916–923. doi:10.1158/1940-6207.CAPR-11-0022.

Clonal Structure of Carcinogen-induced Intestinal Tumors in Mice

Andrew T. Thliveris[1,9], **Linda Clipson**[2], **Alanna White**[2], **Jesse Waggoner**[2], **Lauren Plesh**[3], **Bridget L. Skinner**[3], **Christopher D. Zahm**[3], **Ruth Sullivan**[4,8], **William F. Dove**[2,5,8], **Michael A. Newton**[6,7,8], and **Richard B. Halberg**[3,8,10]

[1] Department of Ophthalmology and Visual Sciences, University of Wisconsin–Madison, Madison, Wisconsin, USA

[2] Department of Oncology, University of Wisconsin–Madison, Madison, Wisconsin, USA

[3] Division of Gastroenterology and Hepatology, Department of Medicine, University of Wisconsin–Madison, Madison, Wisconsin, USA

[4] Research Animal Resource Center, University of Wisconsin–Madison, Madison, Wisconsin, USA

[5] Laboratory of Genetics, University of Wisconsin–Madison, Madison, Wisconsin, USA

[6] Department of Statistics, University of Wisconsin–Madison, Madison, Wisconsin, USA

[7] Department of Biostatistics and Medical Informatics, University of Wisconsin–Madison, Madison, Wisconsin, USA

[8] UW Carbone Cancer Center, University of Wisconsin–Madison, Madison, Wisconsin, USA

[9] Surgery Service, William S. Middleton Memorial Veterans Hospital, Madison, Wisconsin, USA

Abstract

Previous studies have demonstrated that intestinal tumors from *Apc*$^{Min/+}$ (Min) mice and Familial adenomatous polyposis (FAP) patients are often polyclonal. We sought to determine whether polyclonality is unique to tumors arising from hereditary predispositions or, instead, is a common feature of intestinal tumorigenesis in other pathways to tumorigenesis. Ethylnitrosourea-induced intestinal tumors from mice wildtype at the *Apc* locus and chimeric for the *Rosa26* lineage marker were analyzed. Many were overtly polyclonal, being composed of a mixture of *Rosa26*$^{+}$ and *Rosa26*$^{-}$ neoplastic cells. Statistical analyses revealed that polyclonality could be explained by interactions between two initiated clones separated by a very short distance. The frequency of overtly polyclonal tumors and the range of interactions estimated in this model are similar to those observed when analyzing familial tumors from Min mice. Thus, polyclonality does not depend on the familial pathway to tumorigenesis. Interactions between two initiated clones might provide a selective advantage during the early stages of intestinal tumorigenesis.

Keywords

Tumor clonality; tumorigenesis; colon cancer; aggregation chimera; spatial statistics

[10]Corresponding author: Richard B. Halberg, Mailing address: K4/532 Clinical Science Center, MC 5124, 600 Highland Avenue, Madison, WI 53792, Phone: (608)263-8433, FAX; (608)265-5677, rbhalberg@medicine.wisc.edu.

No Conflicts of Interest.

Introduction

The clonal origin of intestinal tumors is an active area of investigation. Tumors could be monoclonal, being derived from a single progenitor, or alternatively, tumors could be polyclonal, being derived from two or more progenitors. Evidence for polyclonality has been steadily accruing over many years (1–6). Novelli and colleagues analyzed benign colorectal adenomas from a patient who carried a germline mutation in the *Adenomatous Polyposis Coli* (*APC*) gene and who was an XY/XO mosaic (3). Some tumors were overtly polyclonal, being composed of both XY and XO cells. Critics argued this study did not prove that intestinal tumors could be polyclonal because the karyotype was inherently unstable. Thirlwell and colleagues analyzed benign colorectal adenomas from patients with FAP for somatic mutations in *APC* (6). All tumors were polyclonal with adjacent dysplastic crypts carrying different mutations. Thus, the findings from these two studies indicate that familial tumors can be polyclonal.

Mouse models are a tool to better understand the clonal origin of tumors in the mammalian intestine. Merritt and colleagues analyzed benign intestinal adenomas from C57BL/6 (B6) mice that were carrying the *Min* allele of the *Apc* gene and chimeric for Rosa26 expression (4). Several tumors were composed of $Rosa26^{+}$ (blue) and $Rosa26^{-}$ cells (white). In this model, genetic instability was not an issue; clearly, familial tumors can be polyclonal. The authors offered two different mechanisms to explain polyclonality: random collision between two or more existing tumors and clonal interactions (4). These explanations could not be distinguished because the tumor multiplicity was extremely high (3, 4). Thliveris, Halberg, and colleagues analyzed tumors from B6 $Apc^{Min/+}$ (Min) mice that were homozygous for the resistance allele of *Mom1* and chimeric for Rosa26 expression (5). *Mom1* is a semidominant polymorphic modifier that reduces the multiplicity and size of intestinal tumors in Min mice (7); one component of this locus is *Pla2g2a*, which encodes a secretory phospholipase (8, 9). Many early adenomas in these aggregation chimeras were overtly polyclonal even though the probability of two tumors coalescing was significantly reduced. These findings support the hypothesis that polyclonal tumors arise from clonal interactions. Statistical analyses of the chimerism revealed that polyclonality could be explained by interactions between two or three initiated clones occurring over a very short distance (5, 10).

Is polyclonality peculiar to humans and mice with a genetic predisposition to intestinal cancer? Investigators have sought to determine the clonality of intestinal tumors from mice treated with a carcinogen. Ponder and Wilkinson analyzed colon lesions from CBA/Ca⇔B6 aggregation chimeras treated with azoxymethane (11). All dysplastic lesions (55/55) and the majority of adenomas (15/17) that developed were composed of cells derived from a single progenitor. Tatematsu and colleagues analyzed colon lesions from C3H/HeN⇔BALB/c aggregation chimeras treated with 1,2-dimethlhydrazine (12). The majority of adenomas (90/91) and the majority of adenocarcinomas (107/119) were monoclonal. The authors argued that the few heterotypic tumors that did form appeared to arise from the random collision because cells from different lineages were arranged in discrete areas rather than intermingled. These two studies had limitations: 1) the aggregation chimeras were composed of cells with significantly different susceptibilities to the carcinogen e.g., CBA mice treated with azoxymethane developed 9 times more lesions than B6 mice, and 2) patch size was large so individual tumors would be homotypic even if derived from multiple progenitors. Griffiths and colleagues analyzed colon lesions from C3H mice mosaic for the expression of glucose-6-phosphate dehydrogenase (13). Colons were rolled, sectioned at eight to ten levels, and stained. The majority of the tumors (27/28) were composed of cells derived from a single progenitor. The authors, however, acknowledged that they could not rule out that a small percentage of tumors are derived from multiple progenitors because only 20% of

crypts were adjacent to crypts with a discordant phenotype. To exclude the possibility that 5% of tumors were polyclonal would have required several hundred tumors to be analyzed.

In this study, we determined the clonality of intestinal tumors in B6 mice treated with ethylnitrosourea (ENU). One of the methods that we employed involved sectioning each tumor *in toto*. Unlike previous studies, we found that many carcinogen-induced tumors can be overtly polyclonal. Statistical analyses were performed to assess likely explanations for the polyclonality, the range of clonal interactions, and the number of contributing clones.

Methods

Mouse Strains and Generation of Aggregation Chimeras

B6 mice and B6 mice heterozygous for the Rosa26 transgene expressing lacZ were obtained from The Jackson Laboratory. Stocks of these strains were maintained by continually backcrossing to B6/J mice (The Jackson Laboratory) that were imported every fifth generation. Offspring were screened for the Rosa26 transgene using PCR assays of DNA isolated from toe clips.

Aggregation chimeras were generated by fusing embryos together from two crosses: B6 $Apc^{+/+}$ x B6 $Apc^{+/+}$ and B6 $Apc^{+/+}$ x B6 $Apc^{+/+}$ $Rosa26^{+}$. Ear snips were also taken from each animal and stained with X-Gal (United States Biological, Swampscott, MA) to ascertain β-galactosidase chimerism. $Apc^{+/+} \Leftrightarrow Apc^{+/+}$ $Rosa26^{+}$ mice were found at the expected ratio.

B6 and B6 $Apc^{+/+} \Leftrightarrow Apc^{+/+}$ $Rosa26^{+}$ were treated with ENU to induce intestinal tumors. Pregnant females, neonates, or adults received a single intraperitoneal injection. The dose was 250 μg per gram of bodyweight. The treated mice were allowed to age until moribund.

Staining and Serial Sectioning Protocol

Whole mounts of the intestines were prepared and stained with X-Gal as previously described (5). Sections were then postfixed in 10% formalin overnight and stored in 70% ethanol. The full intestinal tract was photographed and tumors were excised. All adenomas were embedded in paraffin, serially sectioned *in toto*, and arrayed as two 5-μm sections per slide. Every tenth slide was counterstained with hematoxylin and eosin. When a more complete analysis was required, additional slides were counterstained with nuclear fast red. A homotypic tumor could be composed of cells from a single progenitor or else from cells from multiple progenitors with the same Rosa26 status, whereas a heterotypic tumor is overtly polyclonal.

Analysis of Chimerism

The pattern of chimerism, which is the size and shape of blue and white patches displayed in the intestine, affects our ability to observe overtly polyclonal tumors. To quantify these patterns, each binary image of the intestine was converted to a distance-map image, which records for each pixel the distance to the closest pixel of opposite color. Such maps were then summarized by two functions; one for each color. Each function is a cumulative distribution function of the distances associated with the specific color, documenting for each distance the proportion of blue (or white) pixels whose distance-map value is no longer than that distance. The distance-map functions carry substantial information about the pattern of chimerism and provide more information regarding the size of blue and white patches than other statistical approaches. Computations were done using the R package EBImage (14) and custom R code (available upon request from the authors, www.r-project.org).

The proportion of blue pixels present in each of the mucosal images gave an over-estimate of the underlying blue proportion owing to imaging artifacts, e.g., blue villi overlaying white crypts increase the estimated proportion blue; but white villi, being translucent, do not decrease the estimate if they overlay blue crypts. To account for this effect, we adjusted the observed blue proportions using a simple linear regression model that was fit to data from five sections on which both mucosal and serosal images were available. We found that the corrected proportion of blue was equal to 0.776 multiplied by proportion of blue that was observed on the mucosal side minus 0.0119.

Statistical Evaluation of the Random Collision Hypothesis

To determine whether the rate of overtly polyconal tumors was consistent with the coalescence of tumors that originate independently and uniformly throughout the intestine, the statistical test of Newton and colleagues was applied (10). This test computes a posterior predictive p-value for each chimeric mouse, measuring the probability associated with the number of overtly polyclonal tumors, computed under the assumption of uniform random collision.

Statistical Evaluation of the Clonal Interactions Hypothesis

The pattern of chimerism described by the distance-map functions was combined with tumor phenotype data to address questions about the nature of clonal interaction using two different models. In both models, the log likelihood was computed – the logarithm of the probability of the observed phenotypes, taken conditionally upon the distance-map data (i.e., randomness in the distance maps themselves is not modeled). Contributions to the log likelihood came from each tumor having an unambiguous phenotype; the associated probability was computed from image data specific to the region where that tumor was located. In the disk model (5), the phenotype probability was derived from the distance-map function. For example, the probability of a homotypic blue tumor is the probability that an initiated clone is blue and the minimum distance to the nearest white clone exceeds a parameter δ. In the simpler “arbitrary-range” model, the probabilities use only the overall proportion of blue and white tissue in each region.

Identification of Apc Mutations

Tumors were analyzed for *Apc* mutations using the *in vitro* synthesis of protein as described previously (15). This assay allows truncating mutations between codons 677 and 1609 to be detected.

Results

Clonality of carcinogen-induced intestinal tumors

Two different approaches were used to determine the clonal structure of carcinogen-induced tumors. B6 mice were treated at different ages with ENU and allowed to age until moribund. Those treated as fetuses, neonates, and adults developed on average 1±1, 5±4, and 21±7 tumors, respectively (Table 1; Kruskal-Wallis Test, p=0.0003). Presumably, this difference in tumor multiplicity reflects the number of cells that could potentially be transformed to initiate tumorigenesis. The clonal structure of each tumor was assessed by scoring the number of *Apc* mutations using the *in vitro* synthesis of protein assay in which two regions of exon 15 were tested for truncations (Table 1 and Figure 1A; Reference 16). We reasoned that three or more truncating mutations in *Apc* are indicative of a polyclonal structure, whereas one or two mutations are indicative of a monoclonal structure. A few tumors (3/145) had three or four mutations. The frequency may be low for two reasons: 1) a small portion of the *Apc* gene was tested, or 2) tumorigenesis may be initiated by mutations in

genes other than *Apc*. Some tumors (6/29) were composed of a mixture of Apc-positive and Apc-negative neoplastic cells as determined by immunohistochemistry (Figure 1B-C). As a control, tumors were analyzed from B6 mice carrying the *Min* allele of *Apc* and lacking mismatch repair activity because they often carry truncating mutations. The majority of tumors (5/7) from the controls had two mutations. These findings indicate that ENU-induced tumors might be polyclonal, but the approach had several limitations and the results are open to alternative interpretations.

We decided to use chimeric mice to determine with more certainty the clonal structure of ENU-induced intestinal tumors. $Apc^{+/+}\Leftrightarrow Apc^{+/+}$ $Rosa26^{+}$ aggregation chimeras were generated, treated as adults with ENU, and allowed to age until moribund. The intestinal tract was removed, stained for β-galactosidase activity, and photographed (Table 2 and Figure 2). In this study, the tissue was typically a roughly equal mixture of $Rosa26^{-}$(white) and $Rosa26^{+}$ (blue) clones. Tumors were excised, embedded in paraffin, and serially sectioned *in toto* (Figure 2). $Apc^{+/+}\Leftrightarrow Apc^{+/+}$ $Rosa26^{+}$ aggregation chimeras that were treated with ENU developed on average 5±4 intestinal tumors with a range from 0 to 9. Many of the tumors (47%) were overtly polyclonal, composed of a mixture of white and blue neoplastic clones as judged by histology in which features indicative of neoplastic transformation were the loss of typical anatomic organization of crypts, in conjunction with cellular atypia of the constituent cells (Table 2 and Figure 2D-E). Therefore, carcinogen-induced tumors, like early familial tumors, can have a polyclonal structure.

The percentage of overtly polyclonal tumors in ENU-treated mice was significantly higher than that observed in Min mice (4, 5). The probability of observing 9 overtly polyclonal tumors out of 19 is only 0.0067 if the underlying rate of overt polyclonality is 22% as reported for familial tumors in Min mice by Thliveris, Halberg, and colleagues in 2005 (5). One possible explanation for the higher percentage of overtly polyclonal tumors could be a different pattern of chimerism, which is the relationship of blue to white tissue that is described in part by assessing the distance between clones derived from the two different lineages (Figure 2F). For example, very small blue and white patches increase the opportunity for comingling of clones of opposite color, even if there is no change in the underlying rate of polyclonality. Binary images were converted to distance maps and then reduced to distance-map functions, in order to summarize the pattern of chimeric patches. This image analysis revealed that the samples in this study had patterns of chimerism similar to those observed in our previous study (Figure 2G) (5). Therefore, the relatively high rate of overtly polyclonal tumors is not explained by changes in the pattern of chimerism.

Random collision versus clonal interactions

Polyclonality could result from the random collision of initiated tumors, which would occur when two or more growing tumors in close proximity coalesce to form a single tumor. A statistical test of the uniform random collision hypothesis (3) shows that the number of overtly polyclonal tumors in these mice is too high to be accounted for by having clones initiate uniformly at random and coalesce when sufficiently close (Table 2, Chimeras 101 and 153, each $p<10^{-4}$). This finding is reasonable because tumor multiplicity was very low in all chimeras treated with ENU.

Another possibility is that polyclonal tumors arise from clonal interactions. By combining tumor phenotype with image data on chimerism, we addressed questions about the possible nature of such interactions. The disk model (1), which is an elementary stochastic model of clonal interaction via recruitment after initiation, allowed us to make a judgment about the spatial extent of clonal interactions. In this model, an initiated clone emerges uniformly at random in the intestine and recruits all clones within distance δ to participate in forming a polyclonal tumor. The probability that the resulting tumor is blue, white, or a mixture of

blue and white dependson the pattern of the chimerism as informed by distance maps. A tumor is blue only if the initiating clone is blue and the distance to the nearest white clone is greater than δ. Each tumor phenotype represents a trinomial observation with the probability determined by the two distance maps corresponding to the section in which the tumor formed and δ. The logarithm of the probability of the observed data, i.e., the log likelihood as a function of δ was plotted (Figure 3 curve). The maximum likelihood estimate for δ is 68μm with a 95% confidence interval of 38 to 121μm. This short distance is roughly the same as the distance between the centers of two adjacent crypts.

Number of participating clones

One restriction of the disk model is that it entails full participation, by recruitment, of all cells within a given distance of an initiated clone. We sought to relax this restriction by considering stochastic models in which an initiated clone participates with some number (ν) of partners during tumor initiation. The most elementary model in this direction does not consider interaction range at all, and simply posits that a tumor is formed by the interaction (not collision) of ν+1 clones sampled uniformly at random from the whole intestine. The likelihood is highest when ν equals 1 (Figure 3). Thus, in the arbitrary-range model, the interaction between merely two initiated clones is sufficient to explain the number of overtly polyclonal tumors observed in ENU- treated mice.

Discussion

Polyclonality is a common feature of early adenomas in the mammalian intestine regardless of the pathway to tumorigenesis (3, 5, 6, 10, this study). We determined the clonal structure of intestinal tumors in mice treated with ENU. Statistical analyses revealed that the high percentage of overtly polyclonal tumors was not consistent with simple random collision of initiated tumors, and that it could be explained by interactions between two initiated clones or by the interaction of many clones within a very small region. The same conclusion was drawn when analyzing familial tumors from Min mice (5). The fact that this structure is a common feature of adenomas supports the hypothesis that polyclonality provides a selective advantage at least during the early stages of tumorigenesis in the mammalian intestine.

The percentage of overtly polyclonal tumors in ENU-treated mice was significantly higher than that observed in Min mice. If polyclonality thwarts the host response to some degree, its prevalence will depend on advantage afforded and the biological context. In Min mice, every cell in the animal is heterozygous for a mutation in *Apc*, and this genotype profoundly affects homeostasis in the intestinal epithelium (17). The resulting elevated expression of β-catenin is associated with decreased proliferation, decreased apoptosis, and decreased enterocyte crypt-villus migration. These changes might abrogate the need for interaction with other initiated clones during tumor establishment and growth. By contrast, in mice treated with ENU, any single initiated clone is completely surrounded by normal clones and consequently might be unable to become established on its own. Consistent with this hypothesis, Allard and colleagues demonstrated that stationary normal cells caused growth inhibition of SV40 transformed derivatives through cell cycle arrest (18).

Polyclonality does not depend on the architecture of crypts in the neonatal intestine. When mice are born, crypts are predominantly polyclonal, but around three weeks of age, they become monoclonal. The conversion is referred to as crypt purification and is poorly understood. Tumors in Min mice form at a very early age, so one might argue that polyclonality simply reflects the architecture of the neonatal crypt. In this study, we were able to explicitly test this possibility because the timing of tumor initiation was dictated by the age at which mice were treated with ENU. Multiple *Apc* mutations were observed in intestinal tumors from neonates or adults treated with ENU and overtly polyclonal tumors

were identified in *Apc*$^{+/+}$⇔*Apc*$^{+/+}$ *Rosa26*$^{+}$ adults treated with ENU. Thus, polyclonal tumors can arise when tumorigenesis is initiated in neonatal or adult intestines.

Interactions between two clones are sufficient to account for the number of overtly polyclonal tumors observed in *Apc*$^{+/+}$⇔*Apc*$^{+/+}$ *Rosa26*$^{+}$ adults treated with ENU. However, we cannot exclude the possibility that multiple initiated clones contribute to a single tumor if the interactions occur over a very short distance. Heterotypic tumors often appear to have multiple discrete blue clones (e.g. the large tumor in Figure 2B-C). To fully understand complexity, two different approaches could be used. The ratio of white to blue tissue could be varied by fusing embryos at different stages rather than fusing together only 4-cell to 8-cell embryos as in this study. Variation in chimerism would allow us to further test the number of participating clones as well as the range of interactions. Alternatively, this issue could be addressed by being able to distinguish multiple lineages, as intestinal tumors might be composed of neoplastic cells from two, three, four, or even more progenitors. When we began this study, Rosa26 was the only lineage marker available, but now a number of different markers are available. Livet and colleagues recently demonstrated that up to 90 different neurons in the brain could be uniquely labeled using a transgene in which the expression of four different fluorescent proteins is stochastic (19). This system has been adapted for the intestine (20). Understanding the complexity is fundamental to discerning how polyclonality could affect cancer prevention and therapeutic strategies. Different clones might respond in different ways to treatment and consequently affect the overall response of a tumor.

The nature of the clonal interactions is unknown. An initiated clone could recruit one or more neighboring clones. Neoplastic cells within a dysplastic crypt might release mitogenic factors that affect cellular proliferation in neighboring normal crypts. Indeed, the normal intestinal epithelium adjacent to tumors is often hyperplastic (21). This change could increase the chance that Apc activity is lost in a neighboring crypt. A mutation might occur in *Apc* because errors during replication are not repaired in the context of high rates of proliferation, or else the wildtype allele might be lost by somatic recombination. Alternatively, two or more initiated clones might cooperate simply because they are juxtaposed. For example, ENU might transform numerous clones, but only those clones in close proximity would be able to alter the microenvironment in a way that is permissive to tumor formation and growth. These possibilities can be distinguished by generating aggregation chimeras in which the components have different susceptibilities to tumorigenesis and comparing the number of overtly polyclonal tumors to the number predicted from the recruitment model and the cooperation model.

Polyclonality might persist as tumors progress. The most recent studies addressing clonal structure of intestinal tumors in mice and humans have analyzed only early adenomas. Min mice develop on average 100 tumors and live 97 days. All tumors in these mice are benign adenomas. In this study, mice treated with ENU developed relatively few tumors and lived up to 300 days. Two tumors in these mice were invasive adenocarcinomas of which one was overtly polyclonal. This observation indicates that advanced tumors can be polyclonal. In 1967, Beutler and colleagues found that the primary colorectal tumor and seven metastatic lesions in the liver of a single patient were heterotypic (22). This finding has been dismissed over the years because the patient developed cancer very early in life. Mouse models are becoming available that will allow persistence of polyclonality during tumor progression to be more rigorously tested. Recently, Hung and colleagues have reported that mice carrying mutations in *Apc* and *KRAS* develop colon tumors that metastasize to the liver (23).

This study does have some limitations. First, we were able to follow only two lineages in the aggregation chimeras that we generated. New animal models are becoming available which

will allow multiple lineages to be followed. Second, it must be recognized that non-uniform but still random collision is difficult to separate from models involving explicit clonal interaction. For example, initiated tumors could cluster spatially owing to some non-uniform field effect; the resulting polyclonality would not have required direct interaction, but would have emerged by response to pre-existing regions of high tumor potential. Finally, we interrogated the observed heterotypic rates and image data in ENU-treated mice using elementary statistical models of tumor formation in order to make some judgments about the nature of clonal interaction in polyclonal tumors. We fully appreciate that the statistical models described are extreme simplifications of the dynamic mechanisms truly at work. As has been found in so many other domains, the use of such simplified models provides a language to discuss primary factors affecting the system (24), and puts a sharper focus on the information content of the available data.

Our analysis of polyclonality in carcinogen-induced intestinal tumors has provided new insights: 1) polyclonality is common in ENU-induced tumors as well as in tumors arising from hereditary predisposition, 2) the formation of polyclonal tumors is independent of the crypt architecture, and 3) statistically, the formation of polyclonal tumors can be explained by the interactions between a pair of clones or even by short range interactions between many initiated clones, but not by the accidental coalescence of growing tumors because of uniform random collision. Since polyclonality is common in two very different pathways to tumorigenesis, further study is clearly warranted. A full understanding of the clonal origin of tumors has the potential to impact cancer prevention and maybe even therapy in the colon.

Acknowledgments

We thank Harlene Edwards and Jane Weeks in Experimental Pathology at the UW Carbone Cancer Center for highly capable technical assistance and Dawn Albrecht, Dustin Deming, Jamie Hadac, Alyssa Leystra, and Terrah Paul Olson for critical review of this manuscript. This paper is dedicated to the memories of Lois Hoeger, Maxine Thering, and Fred Thering.

Financial support: National Cancer Institute Grants R01 CA123438 (RBH), R37 CA63677 (WFD), P30 CA014520 (UW Carbone Cancer Center Core Grant), and start-up funds to RBH from the UW Division of Gastroenterology and Hepatology, the UW Department of Medicine, and the UW School of Medicine and Public Health.

References

1. Beutler E. Multicentric origin of colon carcinoma. Science. 1984; 224:630. [PubMed: 6710162]
2. Hsu SH, Luk GD, Krush AJ, Hamilton SR, Hoover HH Jr. Multiclonal origin of polyps in Gardner syndrome. Science. 1983; 221:951–3. [PubMed: 6879192]
3. Novelli MR, Williamson JA, Tomlinson IP, et al. Polyclonal origin of colonic adenomas in an XO/XY patient with FAP. Science. 1996; 272:1187–90. [PubMed: 8638166]
4. Merritt AJ, Gould KA, Dove WF. Polyclonal structure of intestinal adenomas in $Apc^{Min/+}$ mice with concomitant loss of Apc^{+} from all tumor lineages. Proc Natl Acad Sci U S A. 1997; 94:13927–31. [PubMed: 9391129]
5. Thliveris AT, Halberg RB, Clipson L, et al. Polyclonality of familial murine adenomas: analyses of mouse chimeras with low tumor multiplicity suggest short-range interactions. Proc Natl Acad Sci U S A. 2005; 102:6960–5. [PubMed: 15870186]
6. Thirlwell C, Will OC, Domingo E, et al. Clonality assessment and clonal ordering of individual neoplastic crypts shows polyclonality of colorectal adenomas. Gastroenterology. 2010; 138:1441–54. 54, e1–7. [PubMed: 20102718]
7. Gould KA, Dietrich WF, Borenstein N, Lander ES, Dove WF. *Mom1* is a semi-dominant modifier of intestinal adenoma size and multiplicity in *Min*/+ mice. Genetics. 1996; 144:1769–76. [PubMed: 8978062]
8. Cormier RT, Hong KH, Halberg RB, et al. Secretory phospholipase Pla2g2a confers resistance to intestinal tumorigenesis. Nat Genet. 1997; 17:88–91. [PubMed: 9288104]

9. Cormier RT, Bilger A, Lillich AJ, et al. The *Mom1*^{AKR} intestinal tumor resistance region consists of *Pla2g2a* and a locus distal to *D4Mit64*. Oncogene. 2000; 19:3182–92. [PubMed: 10918573]
10. Newton MA, Clipson L, Thliveris AT, Halberg RB. A statistical test of the hypothesis that polyclonal intestinal tumors arise by random collision of initiated clones. Biometrics. 2006; 62:721–7. [PubMed: 16984313]
11. Ponder BA, Wilkinson MM. Direct examination of the clonality of carcinogen-induced colonic epithelial dysplasia in chimeric mice. J Natl Cancer Inst. 1986; 77:967–76. [PubMed: 3463823]
12. Tatematsu M, Masui T, Fukami H, et al. Primary monoclonal and secondary polyclonal growth of colon neoplastic lesions in C3H/HeN<-->BALB/c chimeric mice treated with 1,2-dimethylhydrazine immunohistochemical detection of C3H strain-specific antigen and simple sequence length polymorphism analysis of DNA. Int J Cancer. 1996; 66:234–8. [PubMed: 8603817]
13. Griffiths DF, Sacco P, Williams D, Williams GT, Williams ED. The clonal origin of experimental large bowel tumours. Br J Cancer. 1989; 59:385–7. [PubMed: 2930703]
14. Pau G, Fuchs F, Sklyar O, Boutros M, Huber W. EBImage – an R package for image processing with applications to cellular phenotypes. Bioinformatics. 2010; 26:979–81. [PubMed: 20338898]
15. Kuraguchi M, Yang K, Wong E, et al. The distinct spectra of tumor-associated *Apc* mutations in mismatch repair-deficient *Apc*^{1638N} mice define the roles of MSH3 and MSH6 in DNA repair and intestinal tumorigenesis. Cancer Res. 2001; 61:7934–42. [PubMed: 11691815]
16. Kuraguchi M, Edelmann W, Yang K, Lipkin M, Kucherlapati R, Brown AM. Tumor-associated *Apc* mutations in *Mlh1*$^{-/-}$*Apc*^{1638N} mice reveal a mutational signature of Mlh1 deficiency. Oncogene. 2000; 19:5755–63. [PubMed: 11126362]
17. Mahmoud NN, Boolbol SK, Bilinski RT, Martucci C, Chadburn A, Bertagnolli MM. *Apc* gene mutation is associated with a dominant-negative effect upon intestinal cell migration. Cancer Res. 1997; 57:5045–50. [PubMed: 9371501]
18. Allard D, Stoker M, Gherardi E. A G2/M cell cycle block in transformed cells by contact with normal neighbors. Cell Cycle. 2003; 2:484–7. [PubMed: 12963849]
19. Livet J, Weissman TA, Kang H, et al. Transgenic strategies for combinatorial expression of fluorescent proteins in the nervous system. Nature. 2007; 450:56–62. [PubMed: 17972876]
20. Snippert HJ, van der Flier LG, Sato T, et al. Intestinal crypt homeostasis results from neutral competition between symmetrically dividing Lgr5 stem cells. Cell. 143:134–44. [PubMed: 20887898]
21. Bjerknes M, Cheng H. Colossal crypts bordering colon adenomas in *Apc*^{Min} mice express full-length Apc. Am J Pathol. 1999; 154:1831–4. [PubMed: 10362808]
22. Beutler E, Collins Z, Irwin LE. Value of genetic variants of glucose-6-phosphate dehydrogenase in tracing the origin of malignant tumors. N Engl J Med. 1967; 276:389–91. [PubMed: 6017245]
23. Hung KE, Maricevich MA, Richard LG, et al. Development of a mouse model for sporadic and metastatic colon tumors and its use in assessing drug treatment. Proc Natl Acad Sci U S A. 107:1565–70. [PubMed: 20080688]
24. McCullagh, P.; Nelder, JA. Generalized linear models. 2. New York: Chapman and Hall; 1989.

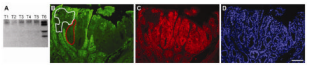

Figure 1.

Some intestinal tumors from ENU-treated mice are polyclonal. Genomic DNA was isolated from tumors and analyzed for mutations in *Apc* (*A*). Many tumors carried no mutations in the two regions of exon 15 that were tested (T1–T5), but occasionally a tumor carried as many as four truncating mutations (T6). The expression of Apc in neoplastic cells within a tumor was sometimes heterogeneous. Apc (*B*) and β-catenin (*C*) were monitored in a single tumor by immunohistochemistry; nuclei were counterstained with DAPI (*D*). When Apc activity is lost, β-catenin translocates from the cell membrane to the nucleus. Most of the neoplastic cells in this tumor displayed this pattern; one example is outlined in red. This is indicative of one mechanism to initiate tumorigenesis in the mammalian intestine. However, some neoplastic cells maintained the expression of Apc and the localization of β-catenin to the membrane; an example is outlined in white. Scale bar = 100 μm.

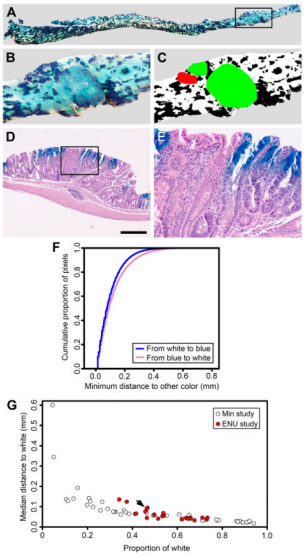

Figure 2.

Some intestinal tumors from ENU-treated aggregation chimeras are overtly polyclonal. Aggregation chimeras were generated and treated as adults with ENU. The mice were sacrificed when moribund and the intestinal tract was removed and stained with X-Gal. Rosa26^{-} cells are white, whereas Rosa26^{+} cells are blue. The entire colon from Chimera 101 is shown (*A*); the outlined area is enlarged in (*B*). Three tumors are evident in the wholemount at higher magnification (*B*) and the digitized image (*C*). Two tumors were overtly polyclonal (green) and one was not scorable (red). Tumor phenotype was determined by examining paraffin sections stained with hematoxylin and eosin (*D*); the outlined area is enlarged in (*E*). In this example, blue and white neoplastic cells are evident at higher magnification (*E*). Distance maps describing the relationship between blue and white tissue in the colon of Chimera 101 were calculated and summarized by cumulative distribution functions (*F*). The intestine from each aggregation chimeras was segmented into five regions. The pattern of chimerism for each region is summarized by the median of the minimum distance to the opposite color, specifically, the median of the distance-map function and compared to the proportion of the reference color (*G*, red circles). The arrow indicates the data for the colon of Chimera 101. Results from very small pieces adjacent to tumors that were used in our previous study involving Min mice (5) are shown for comparison (*A-B*, white-filled circles), and indicate that the pattern of chimerism is not substantially different between the two studies. Note that the wider distribution of samples from the earlier study along the horizontal axis is attributable to size of the very small pieces that were analyzed. Panel *D* scale bar = 500 μm.

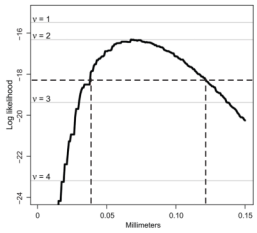

Figure 3.

Two statistical analyses were performed to analyze the pattern of chimerism and to begin to understand the nature of clonal interactions. The log likelihood function for the disk model is shown (curve). This model combines the tumor phenotype data with the image analysis to assess the extent of clonal interactions if an initiated clone can recruit neighboring clones. The maximum likelihood estimate of disk radius is 68μm with a 95% confidence interval of 38 to 121μm (dashed lines). Log likelihoods for an arbitrary-range model of polyclonality are also shown (grey lines labeled ν = 1–4), and indicate that an initiated clone together with one partner (ν=1), randomly drawn from the intestine, provides a parsimonious and well-fitting explanation of tumor phenotypes.

Table 1

Apc mutations in ENU-induced tumors

				Number of tumors carrying N mutations		
Strain	**Age at treatment**	**N of mice**	**Tumor multiplicity, mean ± SD**	**0**	**1–2**	**≥3**
ENU-treated B6 $Apc^{+/+}$ $Msh2^{+/+}$	Fetus	5	1 ± 1	2	0	0
	Neonate	7	5 ± 4	37	0	1
	Adult	9	21 ± 7	91	5	2
B6 $Apc^{Min/+}$ $Msh2^{-/-}$	Adult	8	73 ± 27	2	5	0

Table 2

Clonal structure of ENU-induced tumors in aggregation chimeras.

					N of tumors				
Mouse ID	**Section**	**%blue**	**Median distance to blue, μm**	**Median distance to white, μm**	**Total**	**White**	**Blue**	**Heterotypic**	**Not scorable**
78	C	46	61	55	0	0	0	0	0
95	1	46	75	68	0	0	0	0	0
	2	34	76	45	2	2	0	0	0
	3	34	68	41	0	0	0	0	0
	4	32	55	32	0	0	0	0	0
	C	35	65	41	0	0	0	0	0
101	1	63	78	124	1	0	1	0	0
	2	66	67	135	3	1	1	1	0
	3	53	81	94	0	0	0	0	0
	4	54	60	76	0	0	0	0	0
	C	54	78	90	3	0	0	2	1
105	1	27	114	45	4	1	0	0	3
	2	29	106	45	1	1	0	0	0
	3	36	75	44	0	0	0	0	0
	4	38	53	38	1	0	0	0	1
	C	27	82	38	1	1	0	0	0
153	1	50	59	61	3	0	0	2	1
	2	47	61	53	2	1	0	1	0
	3	54	41	44	0	0	0	0	0
	4	49	44	41	0	0	0	0	0
	C	59	51	64	4	1	0	3	0
				Total:	25	8	2	9	6

Sections 1–4 refer to quarters of the small intestine numbered from proximal to distal; Section C refers to the colon. Some tumors were not scorable because of poor fixation, sectioning, or staining.